

K^+ -nucleus elastic scattering and charge exchange

P. B. Siegel and William B. Kaufmann

Department of Physics, Arizona State University, Tempe, Arizona 85287

William R. Gibbs

Theoretical Division, Los Alamos National Laboratory, Los Alamos, New Mexico 87545

(Received 3 April 1984)

The problem of K^+ -nucleus scattering and charge exchange is treated in a multiple scattering (optical model) formalism. Comparison is made with existing data and fair agreement is found between theory and experiment.

I. INTRODUCTION

The K^+ meson with its relatively weak nuclear interactions has attracted much interest as a probe of the nuclear interior.¹ This promise has been clouded by a persistent discrepancy between theoretical calculations and the best available experimental data. In this paper we address the following questions: (1) How serious is the deviation from experiment? (2) Can nuclear medium effects account for the discrepancy?

As a tool to investigate these issues we use a first-order optical model which was derived from a three-body model. This model, previously applied to pion scattering, incorporates binding, Pauli blocking, recoil, and off-shell effects within a consistent theoretical framework.^{2,7} In brief, our answers to the questions posed are the following: (1) agreement with the existing data on the elastic cross sections is marginally satisfactory provided experimental uncertainties are taken into account; calculated total cross sections are in agreement with experiment⁴ only at the higher energies, and (2) medium effects are significant at roughly the 10% level and are calculable.

At the end of the paper we investigate kaon charge exchange, an important reaction for its potential in studying valence neutron densities. The forward cross section is found to peak at a laboratory kinetic energy of about 220 MeV and reaches a magnitude of about 0.5 mb/sr for a ^{13}C target. The integrated cross section is a mere 0.07 mb for a 200 MeV (laboratory) kaon on a ^{13}C target and falls monotonically as the beam energy increases to 400 MeV.

We begin by briefly reviewing the salient features of the K^+ nucleon system for laboratory momenta below 800 MeV/c. The K^+ interaction is rather weak on the hadronic scale, corresponding to a mean free path in nuclear matter of roughly 5 fm, a typical nuclear size. The implication that multiple scattering (MS) is quite small is confirmed by a comparison of the Born approximation with a full MS calculation as shown in Fig. 1. The correction is seen to be about 50% in contrast to the "correction" to pion scattering of a factor of 5 or 10. Consequently, we are encouraged to describe K^+ nucleus scattering by a first-order optical potential.

There are no clear K^+ -nucleon resonant or bound states

in this energy region, nor are there any inelastic channels with the obvious exception of K^+, K^0 charge exchange on neutrons which we will examine later in this paper. The energy dependence of the cross sections is consequently smooth. Hence, nuclear binding corrections, which act approximately as energy shifts, should be modest. The large medium effects due to annihilation ($\pi NN \rightarrow NN$) and delta resonance formation and propagation, which enliven the π -nucleus system, are totally absent from K^+ -nucleus scattering. At laboratory momenta much higher than 0.8 GeV/c single pion production processes such as $KN \rightarrow K^*N$ and $KN \rightarrow K\Delta$ become important and may complicate the analysis.

Phase shift analyses of the kaon-nucleon system indicate that the s and p waves are most important in this energy regime, but that higher partial waves are essential for precision work. Our approach will be to solve the wave equation which has an optical potential constructed from s - and p -wave kaon-nucleon interactions; higher waves are included through the distorted-wave impulse approximation (DWIA).

Reliable K-N phase shifts are the cornerstone of any analysis of K^+ nuclear data; an accurate determination of these is of first priority in any future experimental K^+ -nuclear program. The most popular set of phase shifts, due to Martin,⁵ fit the rather sparse K^+ -N data quite well. The recent phase shifts of Watts *et al.*⁶ include new data above about 800 MeV/c and are in substantial agreement with Martin's phase shifts. Further data at low energies is needed to more accurately determine the lower energy phase shifts necessary for three-body models.

Summing up, we expect a first-order optical potential with modest medium corrections and with higher K-N partial waves included, at least in the DWIA, to well describe K^+ nuclear scattering in the region below 0.8 GeV/c, provided accurate K^+ -N phase shifts are employed.

In Sec. II we describe the medium corrected optical potential. Section III begins with an analysis of the medium effects, continues with a series of calculations incorporating experimental uncertainties, and concludes with a prediction of charge exchange cross sections. The results are summarized in Sec. IV.

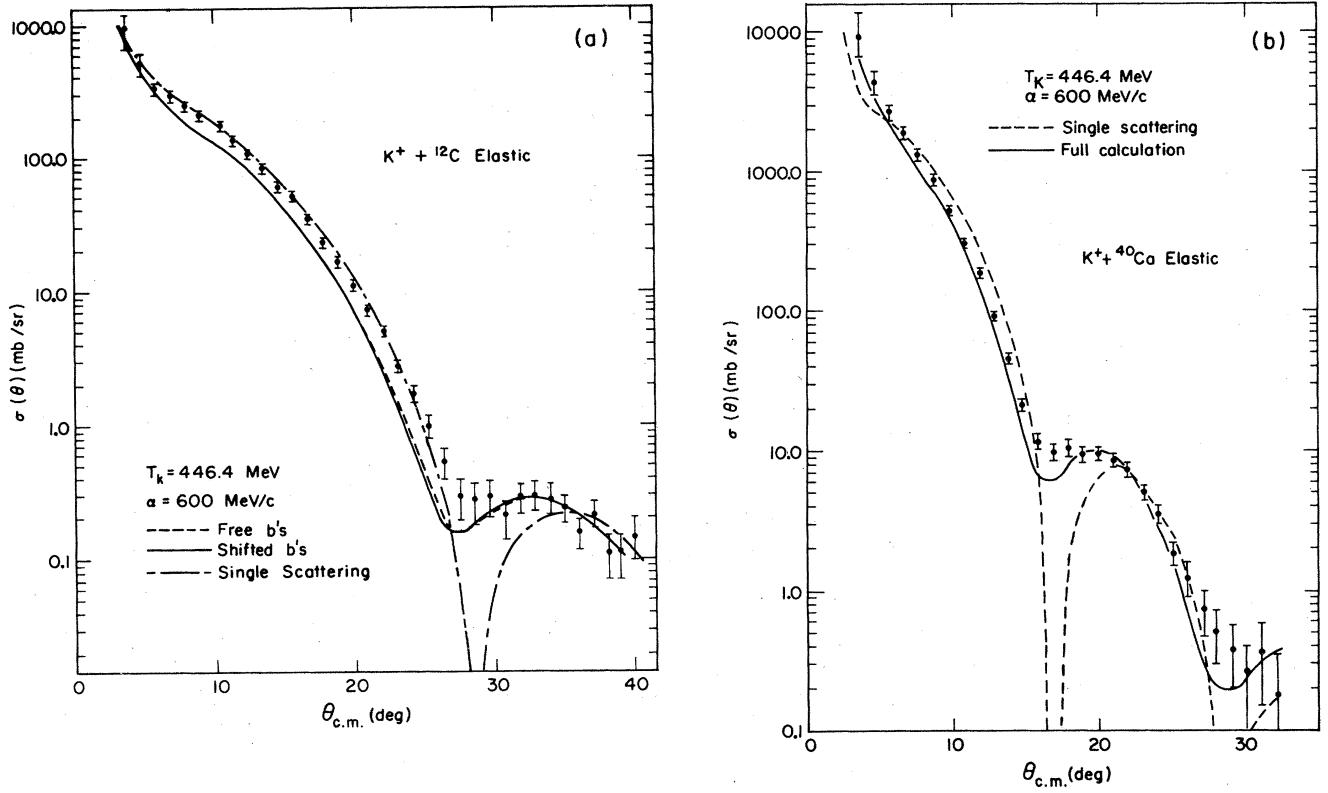


FIG. 1. *Single versus multiple scattering.* Results of a finite range optical model are compared with the single-scattering approximation. Corrections due to medium effects (i.e., energy shifted b 's and finite interaction range) are shown in (a) for ^{12}C and in (b) for ^{40}Ca . Agreement with the data is improved by an overall renormalization (Fig. 3), an angular shift of approximately one degree, and/or lowering of the beam momentum [Figs. 6(a) and (b)].

II. FORMALISM

Our optical potential is based upon a three-body system of kaon (K), nucleon (N), and residual nuclear core (C). This potential was derived in Ref. 7. The major result is

$$\langle \vec{k}' | V(E) | \vec{k} \rangle = \sum_A \sum_{A'} \int d\vec{q}' d\vec{q} \phi_A^*(\vec{q}') \tilde{\phi}_{A'}^*(\vec{q}' + c\vec{k}') \\ \times \langle -a\vec{q}' + b\vec{k}' | t_{KN}(E + E_A - \tilde{E}_{A'}) | -a\vec{q} + b\vec{k} \rangle \tilde{\phi}_{A'}(\vec{q} + c\vec{k}) \phi_A(\vec{q}), \quad (1)$$

where \vec{k} and \vec{k}' are kaon momenta in the kaon-nucleus center-of-mass frame (3 c.m.). $\langle \vec{p}' | t_{KN}(E) | \vec{p} \rangle$ is the kaon-nucleon scattering matrix evaluated in the kaon-nucleon center of mass system (2 c.m.). A , which labels the nuclear state, is summed over occupied nuclear levels and A' summed over all nuclear levels. The effects of Pauli blocking have been calculated by the method introduced in Ref. 2 and were found to be negligible ($< 1\%$) at the energies used in this paper. In a semirelativistic picture the quantities a , b , and c are given, approximately, by

$$a = \frac{\omega_K}{\omega_N + \omega_K}, \quad b = \frac{\omega_N(\omega_K + \omega_N + \omega_C)}{(\omega_N + \omega_C)(\omega_K + \omega_N)}, \quad c = \frac{\omega_C}{\omega_N + \omega_C} \quad (2)$$

with all energies computed in the 3 c.m. The nuclear wave functions are defined as eigenstates of the equations

$$\left[-\frac{\nabla^2}{2\mu} + V_{NC} \right] \phi_A = E_A \phi_A, \quad \mu = \frac{\omega_N \omega_C}{\omega_N + \omega_C} \quad (3a)$$

and

$$\left[-\frac{\nabla^2}{2\eta} + V_{NC} \right] \tilde{\phi}_A = \tilde{E}_A \tilde{\phi}_A, \quad \eta = \frac{(\omega_K + \omega_N)\omega_C}{\omega_K + \omega_N + \omega_C}. \quad (3b)$$

In Eqs. (3) the index A denotes collectively n , the radial quantum number, and l , the orbital angular momentum of the nuclear state. The distinction between E_A and \tilde{E}_A , not made in Ref. 7, provides for the proper transformation between the 2 c.m. and 3 c.m. coordinate frames. The eigenstates ϕ_A and $\tilde{\phi}_A$ are identical when V_{NC} is an infinite square well potential, although the energies differ due to the reduced mass factors. For s and p waves the t matrix is chosen to be

$$\begin{aligned} \langle \vec{p}' | t_{KN}(E) | \vec{p} \rangle &= \frac{-2\pi}{\mu_{KN}} \left[f_0(E) + \frac{f_1(E)}{p_2^2(E)} \vec{p} \cdot \vec{p}' \right] v(p)v(p') \\ &\equiv [b_0(E) + b_1(E) \vec{p} \cdot \vec{p}'] v(p)v(p'), \end{aligned} \quad (4)$$

where $p_2(E)$ is the on-shell kaon momentum in the 2 c.m. and we have defined

$$f_l(E) = (l+1)f_{l+}(E) + lf_{l-}(E),$$

where \pm refers to $j = l \pm \frac{1}{2}$,

$$f_{l\pm}(E) = \frac{\eta_{l\pm} e^{2i\delta_{l\pm}(E)} - 1}{2ip_2(E)}, \quad (5)$$

$$\mu_{KN} = \frac{\omega_K \omega_N}{\omega_K + \omega_N}, \quad v(p) = \frac{\alpha^2 + p_2^2(E)}{\alpha^2 + p^2}.$$

We have used symmetric spin and isospin amplitudes as befits closed shell nuclei with $N=Z$. The reader is referred to the work of Martin⁵ for the spin-isospin analysis and the parametrization of the phase shifts. After partial wave analysis the optical potential becomes, including recoil terms,⁷

$$\begin{aligned} \langle \vec{k}' | V(E) | \vec{k}' \rangle &= \sum_L \left[\frac{2L+1}{4\pi} \right] P_L(\cos\theta) v(bk') v(bk) \sum_{AA'} b_0(E + E_A - \tilde{E}_{A'}) B_{AA'}^L(k, k') \\ &\quad + b_1(E + E_A - \tilde{E}_{A'}) [b^2 D_{AA'}^L(k, k') - ab E_{AA'}^L(k, k') - ab E_{AA'}^L(k', k) + a^2 F_{AA'}^L(k', k)]. \end{aligned} \quad (6)$$

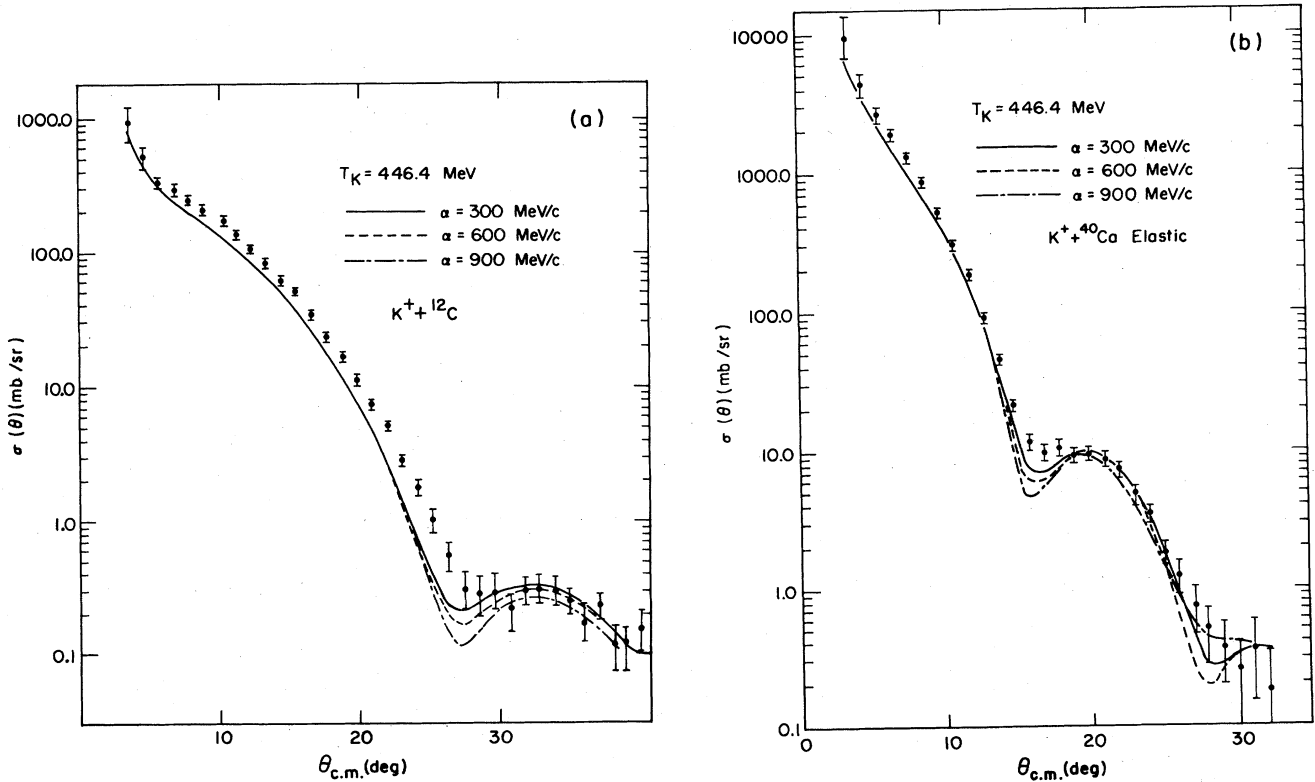


FIG. 2. Cross section dependence on the range of the KN interaction. The parameter describing interaction range of the KN interaction is defined in Eq. (5). The sensitivity to variations in the parameter is greater for larger nuclei [Ca in (b)] than for lighter ones [C in (a)]. In any case the variation is much smaller than for pion scattering.

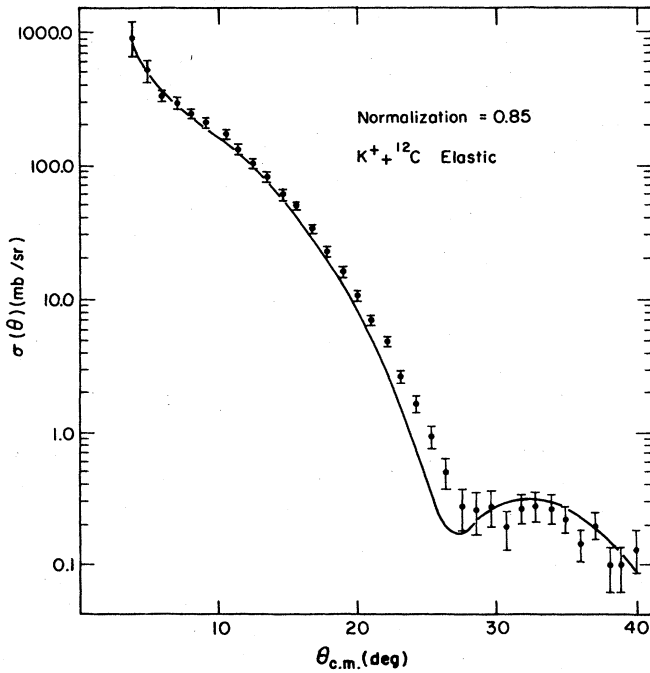


FIG. 3. *Effect of renormalization.* The theoretical cross section corresponding to off-shell range 600 has been multiplied by a factor of (1/0.85) which is consistent with the experimental uncertainty of the data. A similar improvement is seen for the Ca data. See Table I for the corresponding values of χ^2 .

TABLE I. χ^2 per data point.

T_k	$\alpha=600$ MeV/c $\Delta=0^\circ$		^{40}Ca
	N	^{12}C	
446.4	1.0	6.7	3.4
446.4	0.85	3.1	1.6
446.4	0.75	2.2	1.8
425.0	1.0	3.8	1.7
425.0	0.85	1.4	2.8
$\alpha=300$ MeV/c $\Delta=1^\circ$			
433	0.85	1.4	2.3
440	0.85		1.2
440	1.0		0.6

Recoil and energy shifts have been neglected in the off-shell factors $v(k)$. The quantum states of the nuclear single particle levels are denoted by A ($=n, l$) and A' ($=n', l'$). Each term is a product of two factors. The first, e.g., $b_0(E + E_A - \tilde{E}_{A'})$, depends on the KN amplitude and energy spectrum. The second, e.g., $B_{AA'}^L$, depends only upon the nuclear wave functions. The functions B , D , E , and F are given in the appendix of Ref. 7. For example, B is defined by

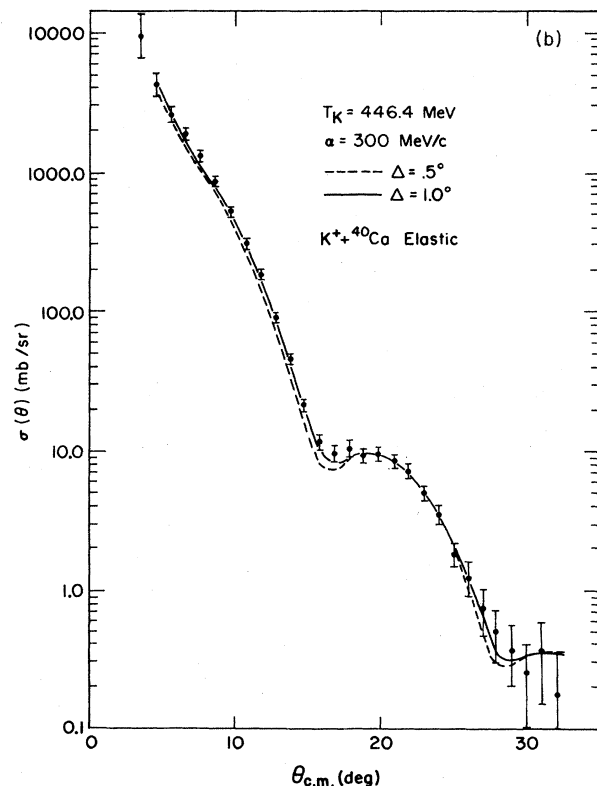
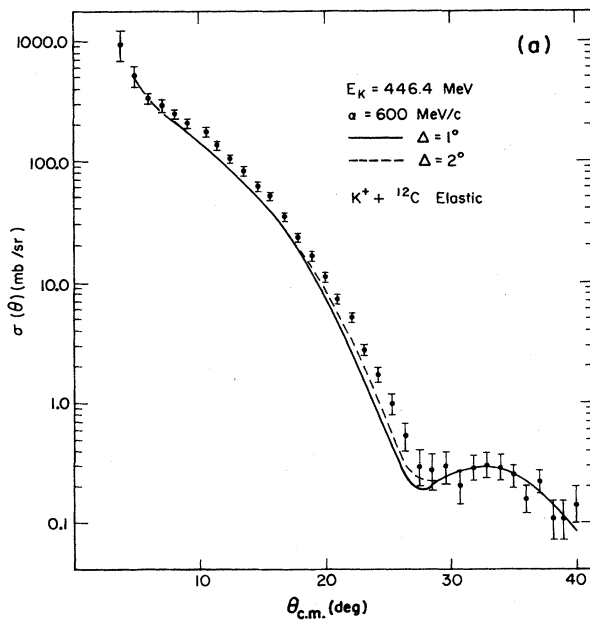


FIG. 4. *Inclusion of angular resolution.* The effect of folding the angular resolution with the theoretical calculation is to partially fill in the cross section at the diffraction dip.

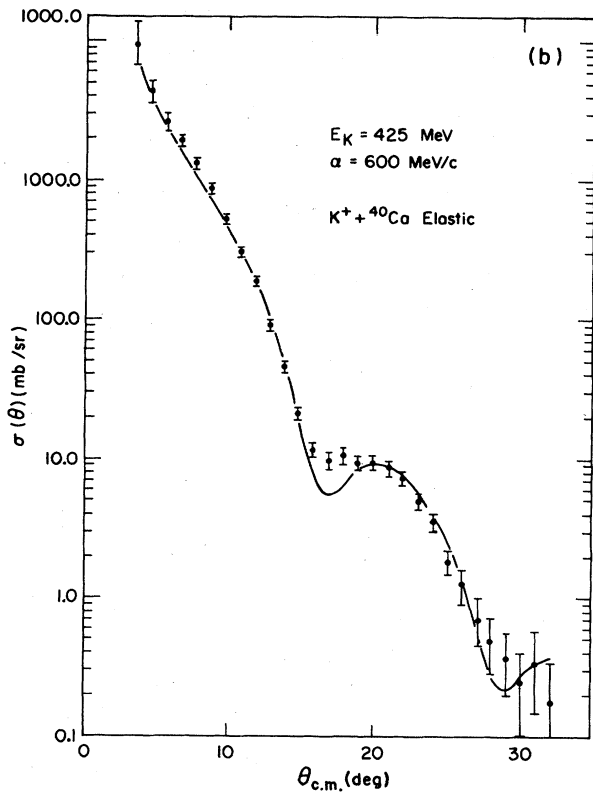
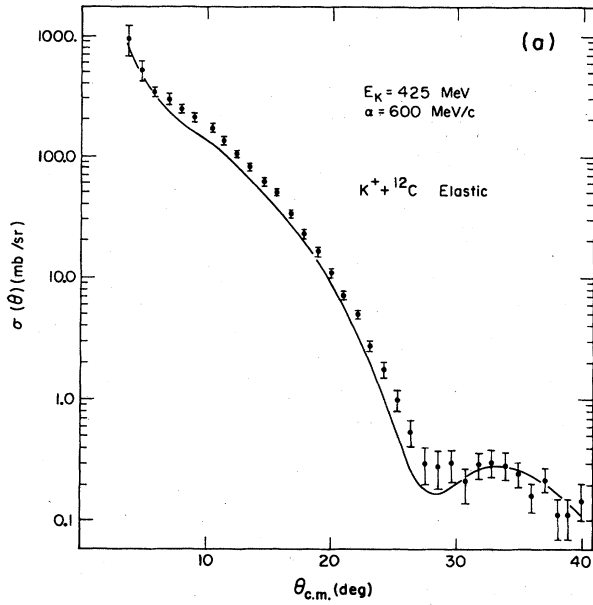


FIG. 5. Effect of variation of beam momentum. The calculation has been done at a beam momentum 3.1% below the nominal experimental value. This corresponds to a laboratory kinetic energy of 425 MeV. The principal effects are to raise the cross section and move the diffraction dip to slightly larger angles.

$$B_{AA'}^L(k, k') = 4\pi C_{000}^{L'L} \Lambda_{AA'}^L(k') \Lambda_{AA'}^L(k), \quad (7)$$

where C is a Clebsch-Gordan coefficient and $\Lambda_{AA'}^L$ is the transition form factor connecting the states A and A' :

$$\Lambda_{AA'}^L(k) = \int_0^\infty r^2 dr j_L(kr) \phi_A(r) \tilde{\phi}_{A'}(r). \quad (8)$$

The complete spectrum of a realistic nuclear well was used in Ref. 7. Here, as in Ref. 2, we have adopted the following simpler procedure: each term in V , such as

$$\sum_{\alpha\alpha'} b_0(E + E_\alpha - \tilde{E}_{\alpha'}) B_{\alpha\alpha'}(k, k'),$$

is written

$$\frac{\sum_{\alpha\alpha'} b_0(E + E_\alpha - \tilde{E}_{\alpha'}) B_{\alpha\alpha'}(k, k')}{\sum_{\alpha\alpha'} B_{\alpha\alpha'}(k, k')} = \bar{b}_0(E, k, k') \sum_{\alpha\alpha'} B_{\alpha\alpha'}(k, k'). \quad (9)$$

The first term, $\bar{b}_0(E, k, k')$, is calculated with a very simple nuclear model, in this case an infinite square well.

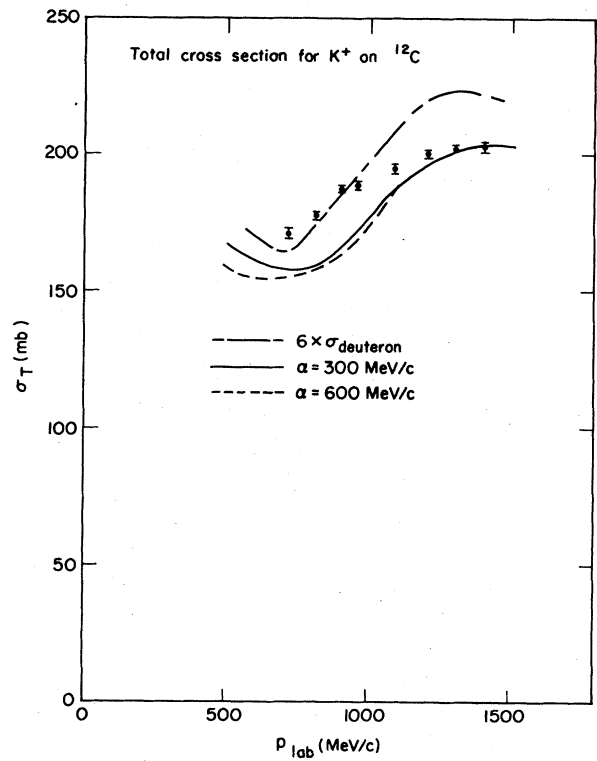


FIG. 6. Total cross section for K - C scattering. The theoretical cross sections have been calculated via the optical theorem after the Coulomb potential has been turned off. The calculated cross section is roughly 10% below the experimental one for p_{lab} in the range 750–1000 MeV/c. It is surprising that the $K^+ + {}^{12}\text{C}$ total cross section exceeds six times that of $K^+ + d$ for p_{lab} in the range 700–900 MeV/c, since one would expect more nuclear shadowing in the former case.

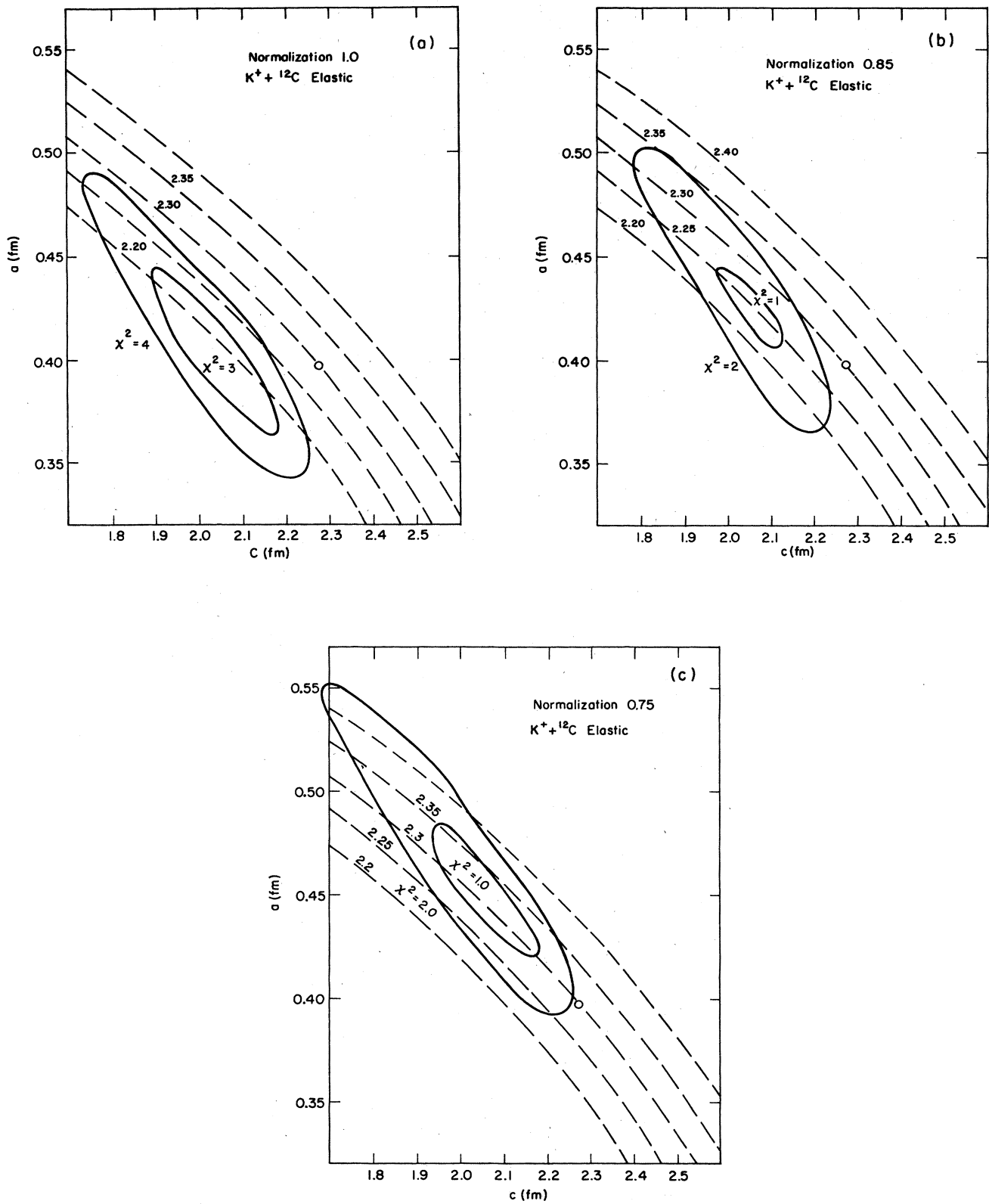


FIG. 7. Dependence of χ^2 on normalization. The iso- χ^2 curves are seen to lie roughly along the constant rms lines so that an rms radius is more accurately determined than the specific values of c and a . A knowledge of normalization is seen to be critical to the determination of the nuclear shape parameters. The axes are labeled by the W - S parameters defined in Eq. (12).

The model dependence is of higher order, largely canceling between numerator and denominator. The error introduced is small as we are making an approximation to an already small correction. The issue was explored for pions (using two very different nuclear models) in our Ref. 2. For the more weakly interacting K^+ the approximation is even better. The momenta k and k' are set to the on-shell value $p_2(E)$ and the off-shell dependence of \bar{b}_0 is subsumed into the v 's of Eq. (5). The second term in Eq. (9) is the ground state nuclear density as was shown in Ref. 2. As the differential cross section is sensitive to this quantity we have computed it with a more accurate nuclear density⁸ to be described later in this paper.

The wave equation to be solved is⁹

$$[-\nabla^2 + 2\mu_N V + p_3^2(E)]\psi = 0, \quad (10)$$

where

$$\mu_N = \frac{\omega_K \omega_N}{\omega_K + \omega_N} \quad (11)$$

is the "kaon reduced energy" with respect to the nucleus and p_3 is the momentum in the 3 c.m. The wave equation was solved in coordinate space⁸ where V is an integral operator obtained from the transform of Eq. (6). V includes an electrostatic potential derived from the charge form factor.¹⁰

The optical potential [Eq. (1)] contains, in principle, contributions from all kaon-nucleon partial waves. Equation (4) includes only s - and p -wave KN interactions. These are by far the most important ones at 800 MeV/ c , where most of our calculations were performed. This suggests splitting the optical potential into $V(s,p)$, given by Eq. (4), and $V(h)$, generated from d and f partial waves for the KN system. (g and higher waves are negligible in the Martin phase shift representation.) In standard DWIA fashion we have used the solution of the wave equation (10) with potential $V(s,p)$ as distorted waves to evaluate the contribution of $V(h)$ to the nuclear scattering amplitude. We find that the differential cross section is increased by about 15% in the angular range 0° – 40° for which data exist. By comparing the contributions of $V(h)$ to the kaon-nuclear amplitude by use of the distorted-wave impulse approximation (DWIA) and plane-wave impulse approximation (PWIA), we estimate the error incurred by our use of the DWIA is probably less than 4%. It would be better, of course, to include the d and f waves exactly, and we intend to do this eventually, but we believe our DWIA method is adequate for present purposes.

III. RESULTS

As mentioned in Sec. II, we have found Pauli blocking of intermediate filled nuclear levels to be negligible at the energies of interest here. We expect such corrections to become important only for laboratory momenta below about 300 MeV/ c .

The off-shell effects due to the finite interaction range of the KN system are expected to be small because, as is seen in Fig. 1, multiple scattering is small. The results of calculations with off-shell ranges of 300, 600, and 900

MeV/ c are given in Fig. 2(a) for ^{12}C and in Fig. 2(b) for ^{40}Ca . In agreement with expectations there is very little off-shell dependence at the forward angles; however, at the minima the variation is significant and must be dealt with. As has been noted by other authors,¹ the calculations lie below the experimental data in the intermediate angular region. The figure shows that this discrepancy is not alleviated by varying the range of the potential. The chi-squared per data point, shown in the first column of Table I, is especially unsatisfactory for ^{12}C .

The large mass of the kaon suggests that recoil effects may be significant. To investigate this we omit the last three ("recoil") terms in Eq. (6). These terms would be absent (i.e., $a = 0$) if the kaon were massless. We find that these terms have little effect until the dip at 28° , in the case of ^{12}C , where they increase the cross section by about 12%. By 50° , beyond the available data, the terms raise the cross section by about 20%. The correction is not larger because it is proportional to b_1 , the K^+ -N p -wave amplitude, whereas the dominant contribution to the optical potential comes from b_0 , the s -wave amplitude.

Since the correspondence with the experimental data is not entirely satisfactory we have explored several avenues to attempt to reconcile theory and experiment:

(1) Marlow *et al.*³ state a normalization uncertainty of 18%. The χ^2 obtained after scaling the data by a factor

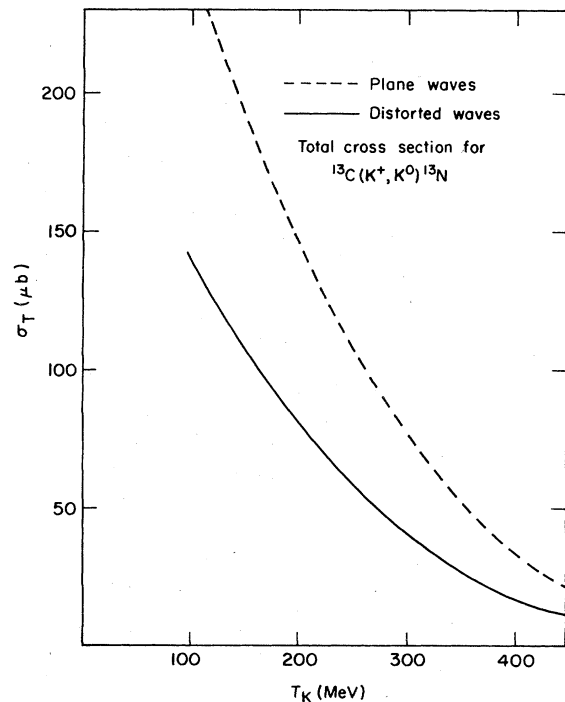


FIG. 8. Integrated charge exchange cross section on ^{13}C . The effect of multiple scattering is to reduce the cross section by a factor of approximately 2. Note the rapid drop in the cross section with energy. The off-shell range parameter is 600 MeV/ c for this calculation and that of Fig. 9.

0.85 is given in Table I. There is a noticeable improvement, especially for carbon, but the theoretical curves remain below the data. See Fig. 3 for which the theoretical curves are divided by 0.85.

(2) In Figs. 4(a) and (b) we have folded our theoretical curves with a Gaussian distribution $\exp[-\frac{1}{2}(\theta/\Delta)^2]$, where Δ is 0.5, 1.0, or 2.0 deg. This is roughly in accord with the angular resolution of the data. The 1 deg smearing tends to improve our fit to the data especially for ⁴⁰Ca between 10° and 20°, but otherwise is not very important. It is critically important to have a precise measurement of the scattering angle in the region of rapid falloff of the cross section. It is interesting to note that a shift of the data (or theory) in angle by less than a degree would result in reasonable agreement without any change in the normalization.

(3) To get a feeling for the sensitivity of the calculation to uncertainties in the beam momentum, curves are shown for an incident momentum of 775 MeV/c (or $T_{\text{lab}}=425$ MeV), 3.1% below the published momentum. See Figs. 5(a) and (b). The net effect is to lower the cross section and slightly increase the angle of the diffraction dip. A 3.1% decrease is unlikely to be the explanation of the present discrepancy since the experimental uncertainty in the beam momentum is estimated to be (1–2%).¹¹ In any case this exercise emphasizes the necessity of a precise knowledge of the beam energy if quantitative conclusions are to be drawn.

(4) If there is significant energy spread in the beam at the center of the target, theoretical predictions could be made more realistic by folding the calculated curves with the experimentalists' best assessment of the beam spectrum within the target. Thus we have averaged the cross section over the energy spread of approximately ± 3 MeV across the target.¹¹ The alterations are not visible to the scale of our plots.

The above discussion indicates how inaccuracies in the normalization, scattering angle, and beam momentum in certain combinations *could* account completely for the discrepancy between theory and experiment. The parameter values in the lower part of Table I lie entirely within the experimental uncertainties¹¹ but give a very satisfactory χ^2/N . On the theoretical side, the major uncertainties are the range of the KN interaction, the nuclear density (for which we have used a body density derived from the charge density as revealed by electron scattering), and the accuracy of the input KN phases. As remarked earlier, it is essential for us to have complete confidence in the input phase shifts if we are to use this technique for a study of hadronic single particle densities.

Total cross sections are obtained from the optical theorem after first turning off the Coulomb interaction. The results are compared with experiment⁴ in Fig. 6.

Next we will assess the prospects of learning the shape of the single-particle nuclear density from K⁺ nuclear scattering. Other studies by Cotanch and Tabakin¹² and by Coker, Hoffmann, and Ray^{13,14} indicate that the K⁺ is superior to protons for probing the central regions of the nucleus. Here we will attempt to determine the sensitivity of the differential cross section to parameters such as the mean radius, the half-density radius, and the diffusivity of

the surface.

Even if the theory were perfect neither the K⁺ nucleon phase shifts nor the K⁺ nuclear data are yet sufficiently well determined for a precision mapping of single particle densities. What we can do is *assume* (1) the K⁺ N phase shifts are exactly as given by Martin, and (2) the density is given by a model Woods-Saxon form

$$\rho(r) = \rho_0 / \{1 + \exp[(r-c)/a]\} \quad (12)$$

Since the nuclei we are considering have $N=Z$, we have taken the neutron and proton densities to be equal. The c - a plane forms a convenient palette for studying the nuclear shape within the model. Figure 7 displays curves of constant rms radius on this plane. The "best" fit of the single particle density as determined from electron scattering¹⁰ is represented by the circled point. "Best" in this context means that the height at the secondary maximum and the position of the first dip are correctly reproduced. For scattering through angles of less than 40 deg the resulting form factor is very close to that of electron scattering,¹⁰ where account has been taken of the charge structure of the proton.

In order to investigate the sensitivity of the scattering cross section to the form of the nuclear density we solve the optical model for a given (c,a) and plot the corresponding χ^2 with respect to the data. In this way we develop a χ^2 surface which indicates both the sensitivity of the data to variations in a and c and gives us the pre-

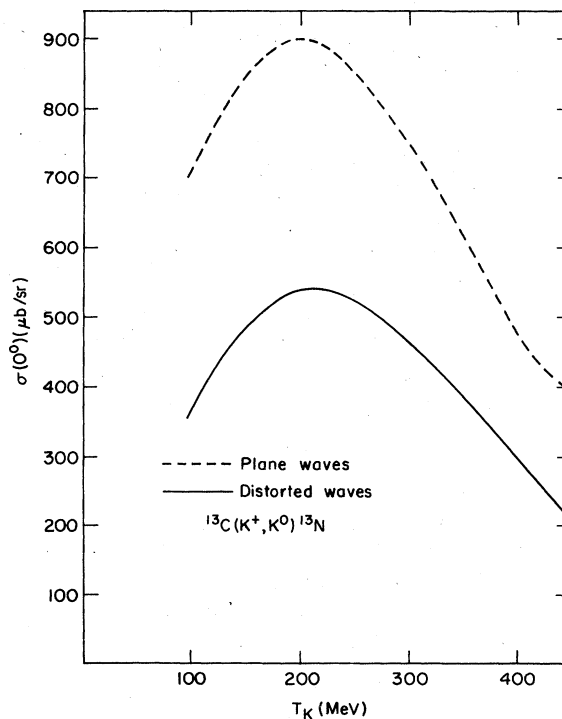


FIG. 9. Forward charge exchange cross section on ¹³C. The effect of multiple scattering is to reduce the cross section by a factor of approximately 2. The peak at 200 MeV laboratory energy is not reflected in the integrated cross section because of the rapidly decreasing nuclear form factor.

ferred values of these parameters. The results of the calculations are plotted in Fig. 7 as iso- χ^2 curves. Near the minima these curves are roughly elliptical in shape with the major axis lying along the lines of constant rms radius. From this we conclude that the rms radius is obtained more easily than the individual values of c and a . A second rather striking result is that the χ^2 minimum occurs at substantially smaller rms radius than for the e^- scattering density. The poorness of our fit indicates that even this qualitative result should be viewed with caution. To test the effect of the normalization uncertainty of 18% we have recalculated χ^2 with the data multiplied by 0.85 and 0.75, which as indicated earlier, greatly improve the quality of the fits. At the same time the predicted rms radii are more in agreement with those of electron scattering. Interestingly, the preferred densities possess a substantially greater diffusivity than the McCarthy-Sick density. We emphasize that the shape parameters found here are not to be taken seriously since the uncertainties in beam normalization and energy must first be clarified and the K^+ phase shifts measured with higher precision.

It should be kept in mind that the body densities obtained from hadron scattering need not *in principle* coincide with those obtained from electron scattering even though the charge form factor of the nucleon has been removed. For example, the neutron distribution may differ from the proton's distribution. Corrections due to interactions of electrons and hadrons with non-nucleonic constituents of the nucleus could also be very different.

We turn finally to charge exchange scattering. As with positive pion single charge exchange, K^+ mesons can transfer a single unit of charge to a nucleus, converting a neutron into a proton. Such processes are potentially excellent probes of the valence neutron wave function. Because of the very large distortion of pion waves in nuclear matter, pion charge exchange is very difficult to analyze. As multiple scattering is far less important for K^+ than for pion scattering, kaonic charge exchange is potentially much easier to analyze theoretically than the corresponding pionic process. Furthermore, the outgoing K^0 meson has a large branching ratio to charged states which aids in its experimental detection. This is of course balanced against the much lower intensity and purity of kaon beams presently available. A machine of the type of LAMPF II (Ref. 13) would remedy this problem.

Figure 8 shows the integrated cross section for K^+, K^0 scattering on ^{13}C . The cross section is disappointingly small and falls rapidly with energy. Figure 9 shows the corresponding forward differential cross section for the process. Two salient points are (1) the cross section peaks at a laboratory energy of about 220 MeV, and (2) the magnitude at the peak is roughly 0.5 mb/sr, a respectable, if not large, size. The calculation has been performed with the DWIA in exactly the same manner as in Ref. 2. A PWIA calculation is also given for comparison. The effect of distortion is to reduce the cross section by roughly a factor of 2. At a laboratory energy of 450 MeV, where nuclear structure studies of the type discussed earlier were attempted, the charge exchange cross section has already dropped a factor of 2 from the maximum to roughly 0.25 mb/sr.

IV. SUMMARY

In this paper we have discussed medium corrections for K^+ -nucleus elastic scattering and single charge exchange for kaon beam momenta of 500–800 MeV/c. Summarizing our main conclusions:

(1) The corrections which cause the major difficulties in pion scattering are much reduced for K^+ scattering. Specifically, Pauli blocking and energy shifts due to the spectrum of intermediate nuclear states have been found to be negligible ($<1\%$). Although small in the forward peak, finite range corrections are seen in Fig. 2 to be significant at and beyond the first minimum of the differential cross section. Recoil corrections are also negligible at small angles but become important by the first minimum.

(2) s - and p -wave K^+ -N interactions dominate the optical potential. d and f waves (collectively) contribute at the 15% level. We find that they may be included through the DWIA with an estimated error of less than 4%.

(3) A relationship between experimental uncertainties and the errors in extracted nuclear shape parameters is indicated in Fig. 7. An accurate knowledge of the overall normalization of the data is seen to be especially important.

(4) When the experimental uncertainties are taken into account there is presently no firm evidence for a discrepancy between the experimental differential cross sections³ and the theory.

(5) The total cross section data⁴ poses an interesting puzzle. See the caption to Fig. 6.

(6) The integrated cross section for single charge exchange, Fig. 8, as would be measured by radiochemical activation experiments, is 5–10 times smaller than the corresponding pion cross section. This is small enough to make such measurements very difficult.

(7) The cross section for forward single charge exchange is roughly the same size as that of pions, so that a " K^0 spectrometer" may be expected to make very useful contributions to an understanding of valence neutron densities.

(8) The distortion effects in single charge exchange decrease the predicted cross sections by roughly a factor of 2 from the PWIA, so they must be treated with some care.

A related work by Chaumeaux and Lemaire¹⁵ has appeared recently.

ACKNOWLEDGMENTS

We thank Prof. F. Tabakin for use of his program which generates the KN amplitudes and Dr. L. Ray for several discussions. Communications with Prof. E. Hungerford, Dr. D. Marlow, and Prof. D. Bugg about the experimental data are also gratefully acknowledged.

APPENDIX

In this appendix we will give an approximate evaluation of the three-body optical potential. The result gives insight into the kinematical aspects of this type of model. The treatment is entirely nonrelativistic.

Our starting point is Eq. (1). The basic approximation in this appendix is the assumption that the intermediate nucleon-core states are free, i.e., plane waves:

$$\tilde{\phi}_m(\vec{q}) \rightarrow \phi_{\vec{p}}(\vec{q}) = \delta(\vec{p} - \vec{q}), \quad (\text{A1})$$

$$\sum_m \rightarrow \int d\vec{p}, \quad E_m \rightarrow \frac{p^2}{2\eta}.$$

This approximation would hold at high incident energies and with weak nuclear binding potentials. Integration over the delta functions gives

$$\langle \vec{k}' | V(E) | \vec{k} \rangle = \int d\vec{q} \phi_0^*(\vec{q} - c\vec{\Delta}) \phi_0(\vec{q}) \left\langle -a(\vec{q} - c\vec{\Delta}) + b\vec{k} \left| t \left[E - \frac{(\vec{q} + c\vec{k})^2}{2\eta} \right] \right| -a\vec{q} + b\vec{k} \right\rangle, \quad (\text{A2})$$

where $\vec{\Delta} = \vec{k}' - \vec{k}$ is the momentum transfer in the 3 c.m. Assuming that the ground state density may be approximated by a Gaussian, $N \exp(-R^2 q^2)$, Eq. (A2) becomes

$$\langle \vec{k}' | V(E) | \vec{k} \rangle = N^2 e^{(-c^2 R^2 \Delta^2 / 2)} \int d\vec{q} e^{-2q^2 R^2} \left\langle -a \left[\vec{q} - \frac{c}{2} \vec{\Delta} \right] + b\vec{k}' \left| t \left[E - \frac{[\vec{q} + \frac{c}{2}(\vec{k} + \vec{k}')]^2}{2\eta} \right] \right| -a \left[\vec{q} + \frac{c}{2} \vec{\Delta} \right] + b\vec{k} \right\rangle. \quad (\text{A3})$$

The effective value at which E is evaluated is

$$E_{\text{eff}} \equiv E - \frac{[\vec{q} + \frac{c}{2}(\vec{k} + \vec{k}')]^2}{2\eta}.$$

As is customary for three-body systems the value of E_{eff} extends down to negative infinity as q tends to infinity. These values are rather unimportant due to the damping factor $\exp(-2R^2 q^2)$ in Eq. (A2). The maximum value of E_{eff} is E and will occur when

$$\vec{q} = \vec{q}_0 \equiv -\frac{c}{2}(\vec{k} + \vec{k}').$$

E , the energy of the kaon in the 3 c.m., is nearly the *laboratory momentum* for all but the lightest nuclei. As a consequence (A3) can include contributions from energies *above* the two-body KN energy usually used in the “ t -rho” approximation to the first order optical potential. The use of a scattering amplitude at this energy may be interpreted as a coherent effect in which the target nucleon recoils as if it were fixed to the residual nucleus.

Such a kinematical situation could lead to a description of coherent pion production below the energy at which pions could be produced off a single nucleon.

To see where contributions to E_{eff} from E may be important, note that if the nuclear size is large, the form factor $\exp(-2q^2 R^2)$ in Eq. (A3) will favor $q = 0$ and hence

$$E_{\text{eff}} \cong E - \frac{c^2(\vec{k} + \vec{k}')^2}{8\eta}. \quad (\text{A4})$$

For forward scattering $\vec{k} = \vec{k}'$, the maximum effective value is

$$E - \frac{c^2 k^2}{2\eta},$$

which is simply the KN kinetic energy in the KN center of mass frame (2 c.m.). It is at this energy that most optical models evaluate the elementary projectile-nucleon amplitude. For *backward* scattering, $\vec{k} = -\vec{k}'$ and the second term in (A4) vanishes. It is thus in the backward direction that the effective energy becomes nearly the *laboratory* energy.

¹The literature may be traced from C. B. Dover and G. E. Walker, Phys. Rep. **89**, 1 (1982). Pauli correlations were estimated by use of the Fermi gas model by C. B. Dover and P. J. Moffa, Phys. Rev. C **16**, 1087 (1977). Binding, finite range, and the “angle transform” corrections are included in M. J. Paèz and R. H. Landau, *ibid.* **24**, 1190 (1981).

²W. B. Kaufmann and W. R. Gibbs, Phys. Rev. C **28**, 1286 (1983).

³D. Marlow, P. Barnes, N. Colella, S. Dytman, R. E. Eisenstein, R. Grace, F. Takeuchi, W. Wharton, S. Bart, D. Hancock,

R. Hackenberg, E. Hungerford, W. Mayes, L. Pinsky, T. Williams, R. Chrien, H. Palevsky, and R. Sutter, Phys. Rev. C **25**, 2619 (1982).

⁴D. Bugg, R. Gilmore, K. Knight, D. Slater, G. Stafford, and E. Wilson, Phys. Rev. **168**, 1466 (1968).

⁵B. R. Martin, Nucl. Phys. **B94**, 413 (1975).

⁶S. Watts, D. Bugg, A. Carter, M. Coupland, E. Eisenhandler, W. Gibson, P. Kalmus, and H. Sanhu, Phys. Lett. **95B**, 323 (1980).

⁷H. Garcilazo and W. R. Gibbs, Nucl. Phys. **A356**, 284 (1981).

- ⁸W. R. Gibbs, B. F. Gibson, and G. J. Stephenson, Jr., *Phys. Rev. Lett.* **39**, 1316 (1977).
- ⁹M. Goldberger and K. Watson, *Collision Theory* (Wiley, New York, 1964), p. 339.
- ¹⁰I. Sick and J. McCarthy, *Nucl. Phys.* **A150**, 631 (1970), (¹²C); J. B. Bellicard *et al.*, *Phys. Rev. Lett.* **19**, 527 (1967), (⁴⁰Ca).
- ¹¹D. Marlow, private communication.
- ¹²S. R. Cotanch, *Phys. Rev. C* **23**, 807 (1981); F. Tabakin, *ibid.* **15**, 1379 (1977).
- ¹³G. W. Hoffman, L. Ray, and W. R. Coker, *Conventional Nuclear Physics at LAMPF II: K⁺-Nucleus Elastic and Inelastic Scattering*, *Physics at LAMPF II*, Los Alamos Report LA-9798-P, 26, 1983; see also, L. Ray, *Nuclear Structure Studies with Kaons at LAMPF II*, *Proceedings of the Third LAMPF II Workshop*, Los Alamos Report LA-9933-C, 419, 1983.
- ¹⁴W. Coker, G. Hoffmann, and L. Ray, *Phys. Lett.* **135B**, 262 (1984).
- ¹⁵A. Chaumeaux and M.-C. Lemaire, *Phys. Rev. C* **28**, 772 (1983).